Effect of the Defect Clusters on the Mobility in Neutron-Irradiated P-type Silicon

Yutaka TOKUDA and Akira USAMI*

中性子照射されたP型シリコンにおける欠陥群の易動度への影響

徳田　豊，宇佐美　晶

abstract

The carrier scattering due to the defect clusters in neutron-irradiated p-type silicon was studied. The spherical cluster model was found to be inadequate to explain the carrier scattering in neutron-irradiated p-type silicon. So, we presented the model about the cluster scattering on the basis of the empirical relation, which is called "empirical model". The scattering cross section per defect cluster A_e and per defect S_e in the empirical model were much larger than those in the spherical model, respectively. S_e was one to two orders of magnitude larger than the scattering cross section per singly charged center. A_e and S_e did not depend on the oxygen concentration and Cu-contamination but only on the acceptor concentration. The acceptor concentration dependence of A_e was not so simple as the spherical model expected. The temperature dependence of the mobility after neutron irradiation in the empirical model was in good agreement with the experimental results over the measurement temperature range 103-322° K in the resistivity range 1-135 ohm-cm. On the other hand, the mobility by the spherical model deviated considerably from the experimental results, especially in the low temperature range. The mobility due to the cluster scattering in the empirical model slightly depended on the temperature and had a tendency to saturate as the temperature decreased in the temperature range 103-157° K, while it depended on $T^{-0.60}$ in the temperature range 164-322° K, which could be explained qualitatively by the cluster-space charge region model. This situation was not true for the spherical model.

1. Introduction

Defect clusters introduced in neutron-irradiated germanium and silicon are expected to act as scattering centers, owing to the width of the space charge regions and the barrier height formed by the cluster-space charge regions and to influence the carrier scattering more strongly than singly charged scattering centers [1]. Wertheim [2] has observed a rapid drop in the mobility at low temperature in neutron-irradiated silicon which cannot be observed in electron-irradiated silicon. He ascribes it to bombardment-induced inhomogeneities. Stein [3), 4)] has reported that the reciprocal mobility-to-carrier removal ratios for the defect clusters in neutron-irradiated silicon are larger than those for singly charged A-centers [5]. This suggests that the scattering cross sections of

*Department of Electronics, Nagoya Institute of Technology.

the defect clusters are larger than those of singly charged centers. Furthermore, Usami and Tokuda [6] has reported that the reciprocal mobility-to-carrier removal ratios for the defect clusters in neutron-irradiated p-type silicon increase as the insulating volumes of the defect clusters increase. This suggests that the scattering cross sections of the defect clusters increase as the insnlating volumes increase. These scattering phenomena cannot be explained by the lattice scattering and charged center scattering which generally cover the mobility behavior in the semiconductor and insulators. Assuming that the configuration of the defect clusters in neutron-irradiated germanium and silicon is spherical, Gossick [1] and Crawford and Cleland [7] have treated theoretically the carrier scattering from the defect clusters. Flanagan [8] has tried to explain the temperature dependence of the mobility in neutron-irradiated germanium and silicon by applying the spherical cluster model [1] to Born approximation.

On the other hand, till now, there have been many reports about such anomalous mobility behaviors in addition to the case of neutron-irradiated germanium and silicon, especially in compound semiconductors [9]. Bube et al. [10] have reported that in insulating GaAs, InP, CdS and CdSe, deep levels are found that have a scattering cross section per defect one to two orders of magnitude greater than that of a Coulombic center. Weisberg [9] has explained the anomalous mobility behaviors, assuming the inhomogeneous distribution of the defects. Such inhomogeneous distribution of defects can cause a localized region to have a charge differing from that of matrix. When this occurs, a surrounding space charge region will form to provide electrical neutrality. He has shown the mobility resulting from scattering from inhomogeneities varies roughly as $T^{-0.5}$.

In the present paper, the authors analyze the carrier scattering due to the defect clusters in neutron-irradiated p-type silicon by using the equation of the mobility resulting from scattering from the space charge regions given by Weisberg [9], which is transformed in section 3 to study the mobility in neutron-irradiated p-type silicon. In 4-a, it is shown that the spherical cluster model is inadequate to explain the carrier scattering in neutron-irradiated p-type silicon. So, in 4-b, the authors present the model about the cluster scattering on the basis of the empirical relation, which is called "empirical model". In these sections, the effects of oxygen and acceptor concentration and Cu-contamination on the carrier scattering is discussed. In, 4-c, the temperature dependence of the mobility calculated by the empirical and spherical models are compared with the experimental results.

2. Experimental Procedure

Electrical conductivity and the Hall effect were measured to obtain the carrier concentration and mobility by the conventional dc method. The silicon samples used in this experiments were boron doped p-type floating zone (FZ) and pulled (CZ) single crystals. The resistivity of the CZ samples was 1, 10 and 100 ohm-cm and the resistivity of the FZ samples was 10 and 135 ohm-cm. The method of Cu-contamination has been described in the previous paper [6] in detail. The characteristics of these samples are presented in Table 1.

Sample code	Crystal growth method	Chemical impurity	Resistivity (ohm-cm)	Total neutron flux (n/cm^2)
A	FZ		135	4.7×10^{12}
A (Cu)	FZ	Cu	135	4.7×10^{12}
B	CZ		100	4.7×10^{12}
B (Cu)	CZ	Cu	100	4.7×10^{12}
C	FZ		10	2.3×10^{13}
D	CZ		10	2.3×10^{13}
E	CZ		1	5.6×10^{14}

Table 1, Properties of boron-doped p-type silicon samples studied in neutron irradiation experiments.

These samples were cut into bridge type by an ultrasonic cutter to measure the Hall effect and the electrical conductivity. Ohmic contacts were obtained by alloying in a H_2 gas flow for 45 min. after aluminum was evaporated in vaccum. The samples were irradiated without enclosing by Cd plating [6] at room temperature in a Rikkyo TRAGA reactor. The neutron flux was about 7.8×10^{10} $n/cm^2\cdot$ sec. The total neutron flux for each sample is presented in Table 1.

3. Theory

Weisberg [9] has given the equation of the mobility μ_s resulting from scattering from the space charge regions, assuming that the current carriers cannot penetrate into the space charge regions and then treating the scattering as a simple collision problem as in gas kinetics. Then, μ_s is given by

$$\mu_s = e\left[N_s\,(2mkT)^{1/2}\cdot A\right]^{-1} \tag{1}$$

where N_s is the concentration of space charge regions, e is the electronic charge, m is the effective mass of the charge carrier, k is Boltzmann's constant, T is the temperature and A is the effective area of the space charge region.

The dominant scattering centers introduced in neutron-irradiated p-type silicon are cluster-space charge regions [6]. Consequently,

$$\Delta(1/\mu) = 1/\mu_i - 1/\mu_o = 1/\mu_c \tag{2}$$

where μ_0 and μ_i are the mobility before and after neutron irradiation, respectively and μ_c is the mobility due to the cluster scattering. The concentration of the defect clusters N_c is obtained by the following equation

$$N_c = \Sigma_v\,\Phi \tag{3}$$

where Σ_v is the probability per cm that a neutron will produce a cluster and Φ is the total neutron flux. When β is the charged defect number per defect cluster, the carrier removal Δp is

$$\Delta p = \beta N_c \tag{4}$$

To study the mobility in neutron-irradiated p-type silicon, eq. (1) is transformed as follows by using eqs. (2), (3) and (4).

$$\frac{\Delta(1/\mu)}{\Delta p} = \frac{(2mkT)^{1/2}}{e}\cdot\frac{A}{\beta} = \frac{(2mkT)^{1/2}}{e}\cdot S \tag{5}$$

where $S=A/\beta$. In eq. (5), A and S mean the scattering cross section per defect cluster snd per defect, respectively. Eq. (5) indicates that the reciprocal mobility-to-carrier removal ratio $\Delta(1/\mu)/\Delta p$ is proportional to the scattering cross section per defect S.

4. Experimental Results and Discussion

4-a. Analysis by the Spherical Model

Gossick [1] has proposed a cluster model in which the configuration of the cluster is spherical. On the basis of the spherical cluster model, one can calculate the average insulating volumes of the defect clusters from the Hall coefficients before and after neutron irradiation [11], [3], [4], [6]. However, not all of the insulating volume is completely insulating since the carriers can penetrate into the outer edges of the defect clusters to a distance for which $e^{\Psi/2kT}$ [1], [7]. Here, Ψ is the barrier height of the defect clusters. Considering the effect of the penetration of the carriers into the outer edges of the defect clusters, Gossick [1] has defined an effective radius r_{eff} of the insulating volumes, which is given by

$$r_{eff} = (r_1 r_2)^{1/2} \tag{6}$$

where r_1 and r_2 are the radius of the disordered regions and the outer boundary of the space charge regions, respectively. So, we define the scattering cross section of the defect clusters as follows

$$A_s = \pi r_{eff}^2 \tag{7}$$

Sample Code	$\Delta(1/\mu)/\Delta p$ (V・sec・cm)	A_s (cm^2)	S_s (cm^2)	A_e (cm^2)	S_e (cm^2)	πr_2^2 (cm^2)
A	2.19×10^{-18}	3.22×10^{-10}	1.57×10^{-11}	1.76×10^{-8}	8.24×10^{-10}	5.30×10^{-9}
A (Cu)	2.32×10^{-18}	3.25×10^{-10}	1.54×10^{-11}	1.71×10^{-8}	8.09×10^{-10}	5.37×10^{-9}
B	1.31×10^{-18}	2.96×10^{-10}	1.13×10^{-11}	9.85×10^{-9}	4.07×10^{-10}	4.46×10^{-9}
B (Cu)	1.21×10^{-18}	2.95×10^{-10}	1.11×10^{-11}	1.00×10^{-8}	4.14×10^{-10}	4.43×10^{-9}
C	1.08×10^{-19}	1.62×10^{-10}	3.88×10^{-12}	1.72×10^{-9}	4.12×10^{-11}	1.34×10^{-9}
D	1.19×10^{-19}	1.62×10^{-10}	3.92×10^{-12}	1.72×10^{-9}	4.04×10^{-11}	1.34×10^{-9}
E	5.81×10^{-20}	9.78×10^{-11}	1.36×10^{-12}	1.41×10^{-9}	1.93×10^{-11}	4.87×11^{-10}

Table 2, Carrier scattering cross section per defect cluster and per defect at 157°K by the spherical and empirical models for various kinds of samples. Each is the mean value of some samples.

Here, subscript "s" means the spherical model. This definition of the scattering cross section of the defect clusters is not inconsistent with the concept of the scattering cross section given by Weisberg [9].

In Table 2, $\Delta(1/\mu)/\Delta p$, A_s and S_s as $r_1 = 250A$ [12] are shown for various kinds of samples. Here, r_2 is calculated from the insulating volumes and β from the carrier removal [6]. The measurement temperature is 157°K. A_s and S_s are found to be independent of both the oxygen concentration and Cu-contamination. This result corresponds well to the fact that $\Delta(1/\mu)/\Delta p$ is independent of both the oxygen concentration and Cu-contamination. A_s decreases as the acceptor concentration increases since the outer layer of the space charge region decreases.

In Fig. 1, $\Delta(1/\mu)/\Delta p$ is shown as a function of S_s. The measurement temperature is 157° K. Dotted line is described according to eq. (5). Full line is the experimental result and its meaning will be discussed in the following section in more detail. From Fig. 1, $\Delta(1/\mu)/\Delta p$ calculated by using eq. (5) is found to be much smaller than that obtained by experiments. This suggests that the scattering cross section per defect cluster obtained by eq. (7) is underestimated. Furthermore, it should be noted that $\Delta(1/\mu)/\Delta p$ is not proportional to S_s. $\Delta(1/\mu)/\Delta p$ increases rapidly above $S_s = 4\times10^{-12}$ cm^2 ($\rho = \sim 10$ ohm·cm), while $\Delta(1/\mu)/\Delta p$ increases slowly in the range from $S_s = 1.36\times10^{-12}$ ($\rho = \sim 1$ ohm·cm) to $S_s = 4\times10^{-12}$ cm^2 ($\rho = \sim 10$ ohm·cm). One possible explanation about the deviation between experiments and theory is that the spherical model is suspicious. Holmes [13] has reported that a spherical defect cluster is not adequate to explain the doping dependence of carrier removal in neutron damaged silicon. Another explanation is that neutrons have energy spectrum since irradiation is performed by reactor neutron, that is, there may be the distribution of the dimention of the disordered region. These factors make it difficult to treat the carrier scattering in neutron-irradiated silicon. In the following section, we estimate the scattering cross section per defect cluster on the basis of the empirical relation.

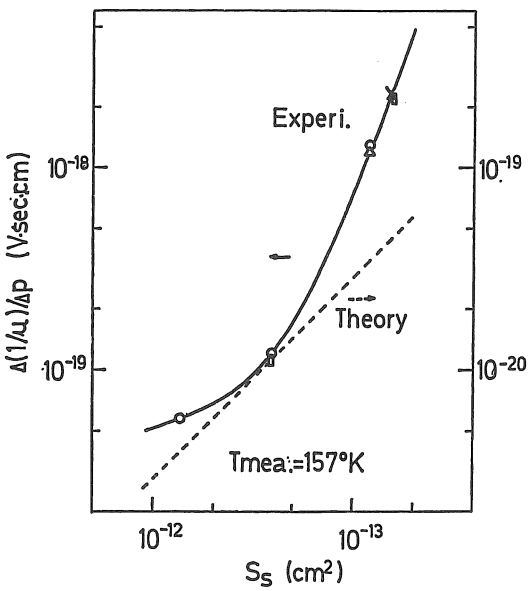

Fig. 1, $\Delta(1/\mu)/\Delta p$ vs. S_s for various kinds of samples. The measurement temperature is 157°K. Full line is the experimental result and dotted line is described according to eq. (5).

○, : noncontaminated CZ samples.
△, : Cu-contaminated CZ samples.
□, : noncontaminated FZ Samples.
×, : Cu-contaminated FZ samples.

4-b. Analisis by the Empirical Model

Full line in Fig. 1 is described according to the empirical equation which fits

the experimental result at 157° K. This empirical equation is given by

$$\frac{\Delta(1/\mu)}{\Delta p}=6.96\times10^{12}S_s^{2.82}+1.14\times10^{-16}S_s^{0.28} \quad (8)$$

From eqs. (1) and (8), the scattering cross section of the defect clusters is given by

$$A_e=\beta(2.39\times10^{21}S_s^{2.82}+3.92\times10^{-8}S_s^{0.28}) \quad (9)$$

Here, subscript "e" means the empirical model. Eq. (9) indicates the relation between the actual scattering cross section per defect cluster and the scattering cross section per defect cluster in the spherical model. In Table 2, A_e and S_e are shown for various kinds of samples. A_e is found to be much larger than the geometrical cross section πr_2^2 in the spherical model. This fact also suggests that the spherical model is inadequate to explain the carrier scattering in neutron-irradiated p-type silicon. A_e and S_e do not depend on the oxygen concentration and Cu-contamination but only on the acceptor concentration. This result coincides with the concept of the defect cluster. To study the acceptor concentration dependence of A_e in detail, A_e is calculated empirically in the range from $N_a=5\times10^{13}$ cm^{-3} to $N_a=1.5\times10^{16}$ cm^{-3}. Then, we use the relation that the insulating volumes in the spherical model decrease with the 0.72 power of the acceptor concentration and the carrier removal rates increase with the 0.23 power of the acceptor concentration [6]. To compare with A_e, A_s is also calculated. In Fig. 2, A_e and A_s are shown as a function of the acceptor concentration. A_s decreases with the 0.24 power of the acceptor concentration. On the other hand, the acceptor concentration dependence of A_e is not so simple as A_s. A_e decreases in the range from $N_a=5\times10^{13}$ cm^{-3} to $N_a=2\times10^{15}$ cm^{-3}. One can understand this result qualitatively by the cluster-space charge region model. However, A_e is almost constant in the range from $N_a=5\times10^{15}$ cm^{-3} to $N_a=1.5\times10^{16}$ cm^{-3}. This seems to mean that in this range of the acceptor concentration, the outer layer of the space charge region is very small compared to the inner layer of the space charge region, that is, the scattering cross section per defect cluster can be determined nearly by the inner layer of the space charge region.

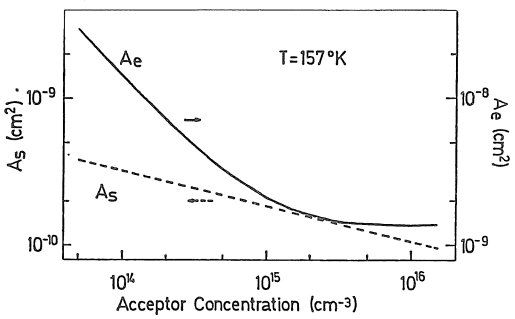

Fig. 2, Acceptor concentration dependence of A_e and A_s at 157°K. Full line and dotted line are calculated by the empirical and spherical models, respectively.

The scattering cross section per singly charged center can be estimated roughly by equating the Coulomb attraction energy to the thermal energy of carriers [10]. Then, it was about 10^{-12} cm^2 at 157° K. From Table 2, S_e is found to be one to two orders of magnitude larger than the scattering cross section per singly charged center. Such larger scattering cross section per defect has been observed by Bube et al [10].

4-c. Temperature Dependence of the Mobility After Neutron Irradiation

In the preceding section, we have presented the empirical model which can explain the mobility at 157° K in neutron damaged p-type silicon. Extending the empirical model to all measurement temperature range (103-322° K), we investigate whether the empirical model can explain the temperature dependence of the mobility after neutron irradiation. To compare with the mobility by the empirical model, we also calculate the mobility by the spherical model. To test the empirical and spherical models, we calculate the mobility for Cu-contaminated FZ 135 ohm • cm, CZ 10 ohm • cm and CZ 1 ohm • cm samples. The mobility μ_i is calculated by eq • (2). Here, μ_0 is given by the experimental values of the mobility before irradiation.

In Fig. (3), the mobility μ_i by the empirical and spherical models for Cu-contaminated FZ 135 ohm • cm sample are shown as a function of the temperature. The total flux is 4.7×10^{12} n/cm^2. Full line and dotted line show the mobility μ_i by the empirical and spherical models, respectively. The experimental values of the mobility after neutron irradiation are shown as open circles. It can be seen from Fig. 3 that the mobility μ_{ie} by the empirical model is in good agreement with the experimental values of the modility over the measurement temperature range within experimental errors. However, the mobility μ_{is} by the spherical model deviates considerably from the experimental values, especially in the low temperature range and is larger than that by the empirical model over the measurement temperature range. The difference between the mobility μ_i by the empirical and spherical models becomes gradually smaller as the temperature increases since the phonon scattering becomes dominant.

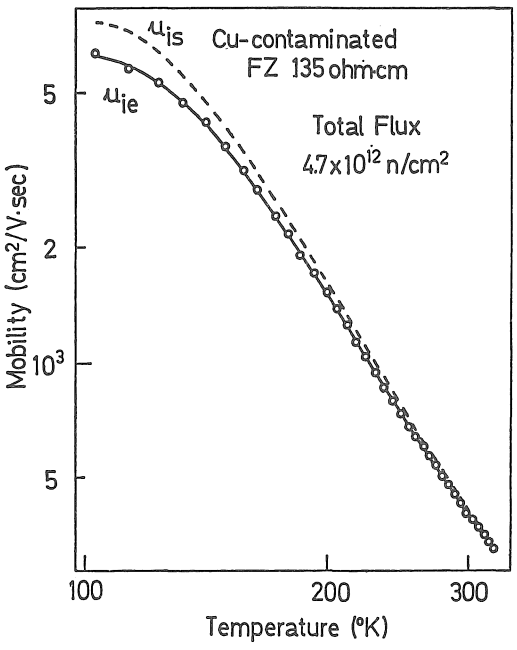

Fig. 3, Temperature dependence of the mobility after neutron irradiation for Cu-contaminated FZ 135 ohm • cm sample. Full line and dotted line show the mobility μ_i by the empirical and spherical models, respectively. The experimental values are shown as open circles.

In Fig. 4, the mobility μ_c by the empirical and spherical models for the same sample in Fig. 3 are shown as a function of the temperature. It is noted that the mobility μ_{cs} is much larger than the mobility μ_{ce} over the measurement temprature range. That is why the spherical model cannot explain the mobility drop after neutron irradiation. Furthermore, the temperature dependence of μ_{cs} is different from that of μ_{ce}. In the temperature range 103-157° K, μ_{cs} depends on $T^{-0.46}$, while in the temperature range 199-322° K, it slightly depends on the temperature. In contrast with μ_{cs}, in the temperature range 103-157° K, μ_{ce} slightly depends on the temperature

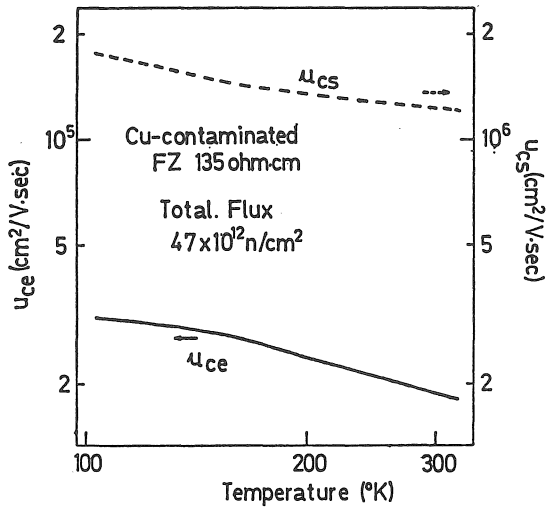

Fig. 4, Temperature dependence of the mobility μ_c due to the cluster scattering by the empirical and spherical models for the same sample in Fig. 4. Full line and dotted line show the mobility μ_c by the empirical and spherical models, respectively.

and has a tendency to saturate as the temperature decreases, while in the temperarure range 164-322° K, it depends on $T^{-0.60}$. As seen from eq·. (1), the mobility μ_c depends on the product of $T^{-0.5}$ and the inverse temperature dependence of A. Therefore, in the temperature range 164-322° K, A_e hardly depends on the temperature. This is due to the reason that in this temperature range, the acceptors fully ionize, that is, the outer layer of the space charge region is independent of the temperature. As expected from the cluster-spsce charge region model, when the acceptors begin to deionize in the low temperature, A_e will begin to increase. In fact, in the temperature range 103-157° K, A_e increased as the temperature decreased. This leads to the result that in the temperature range 103-157° K, μ_{ce} has a tendency to saturate as the temperature decreases. As seen from Fig·4, evidently this situation is not true for the spherical model.

In Fig·5, the mobility μ_i by the empirical and spherical models and observed experimentally for CZ 10 ohm·cm sample are shown as a function of the temperature. The total flux is 2.3×10^{13} n/cm^2. The mobility μ_{ie} by the empirical model is found to be in good agreement with the experimental values of the mobility after irradiation. However, the mobility μ_{is} by the spherical model is larger than that by the empirical model, especially in the low temperature range.

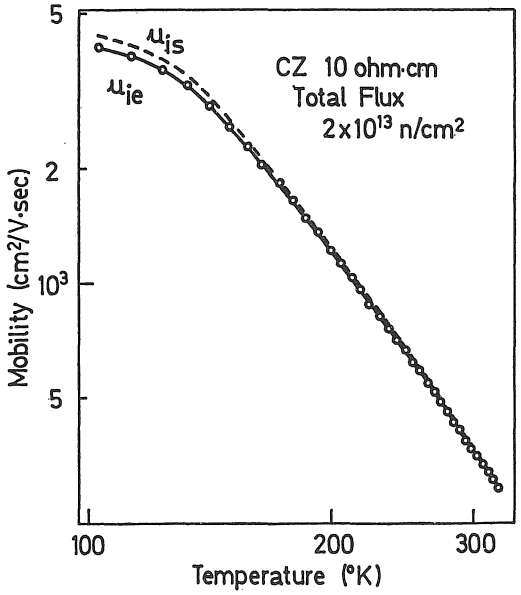

In Fig·6, the results for CZ 1 ohm·cm sample are shown as a function of the temperature. The total flux is 5.6×10^{14} n/cm^2. This flux is relatively larger so that the mobility drop is observed at high temperature in addition to low temperature. The mobility μ_{ie} by the empirical model is in good agreement with the experimental values of the mobility as similar to the results for Cu-contaminated FZ 135 ohm·cm and CZ 10 ohm·cm samples. However, the mobility μ_{is} by the spherical model is larger than that by the empirical model.

Fig.5, Temperature dependence of the mobility after neutron irradiation for CZ [10 ohm • cm sample. Full line and dotted line [show the mobility μ_i by the empirical and spherical models, respectively. The experimental values are shown as open circles.

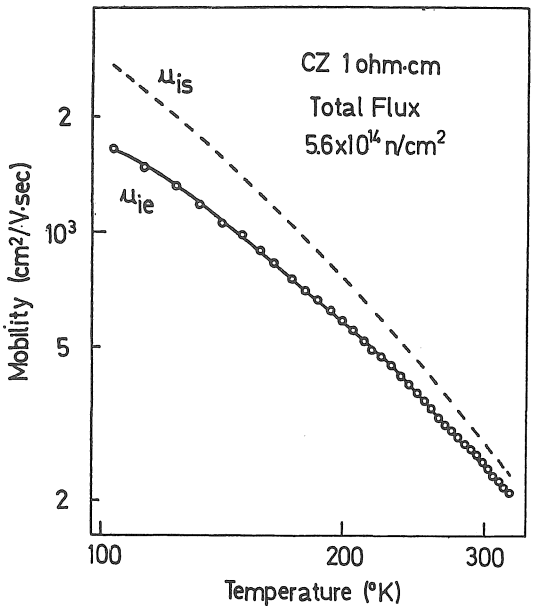

Fig.6, Temperature dependence of the mobility after neutron irradiation for CZ 1 ohm • cm sample. Full line and dotted line show the mobility μ_i by the empirical and spherical models, respectively. The experimental values are shown as open circles.

5. Summary and Conclusion

The spherical cluster model could not explain the mobility drop at 157 °K after neutron irradiation. Furthermore, the spherical model could not satisfy the linear relationship of $\Delta(1/\mu)/\Delta p$ vs. S as expected from eq. (1). So, we estimated the scattering cross section per defect cluster on the basis of the empirical relation. A_e and S_e were much larger than A_s and S_s, respectively. S_e was one to two orders of magnitude larger than the scattering cross section per singly charged center. A_e and S_e did not depend on the oxygen concentration and Cu-contamination but only on the acceptor concentration. The acceptor concentration dependence of A_e was not so simple as the spherical model expected. A_e decreased in the range from $N_a=5\times10^{13}$ cm^{-3} to $Na=2\times10^{15}$ cm^{-3}, while A_e was almost constant in the range from $N_a=5\times10^{15}$ cm^{-3} to $N_a=1.5\times10^{16}$ cm^{-3}. This result could be understood qualitatively by the cluster-space charge region model.

To test the empirical model, the temperature dependence of the mobility after neutron irradiation was calculated for Cu-contaminated FZ 135 ohm • cm, CZ 10 ohm • cm and CZ 1 ohm • cm samples. To compare with the mobility by the empirical model, the mobility by the spherical model was also calculated. The mobility by the empirical model was found to be in good agreement with the experimental values of the mobility after neutron irradiation over the measurement temperature range. However. the mobility by the spherical model deviated considerably from the experimental values, especially in the low temperature range and was larger than that by the empirical model over the measurement temperature range. The mobility due to the cluster scattering was discussed in detail for Cu-contaminated FZ 135 ohm • cm sample. The mobility due to the cluster scattering in the empirical model slightly depended on the temperature and had a tendency to saturate as the temperature decreased in the temperature range 103-157° K, while it depended on $T^{-0.60}$ in the temperature range 164-322° K. These results could be explained qualitatively by the cluster-space charge region model. However. this situation was not true for the spherical model.

Acknowledgements

The authors would like to express their thanks to prof. H. Takematu of the Aichi Institute of Technology and to prof. Y. Inuishi of the Osaka University for their encouragement during this work and to prof. K. Takami of the Rikkyo Nuclear Lab. for neutron irradiation.

References

1) B. R. Gossick : J. Appl. Phys. 30, 1214 (1959)
2) G. K. Wertheim : Phys. Rev. 111, 1500 (1958)
3) H. J. Stein : Phys. Rev. 163, 801 (1967)
4) H. J. Stein : J. Appl. Phys. 39, 5283 (1968)
5) H. J. Stein and F. L. Vook : Phys. Rev. 164, 790 (1967)
6) A. Usami and Y. Tokuda : J. Appl. Phys. 45, 2823 (1974)
7) J. H. Crawford and J. W. Cleland : J. Appl. Phys. 30, 1204 (1959)
8) T. M. Flanagan : IEEE Trans. NS-15, 42 (1968)
9) L. R. Weisberg : J. Appl. Phys. 33, 1817 (1962)
10) R. H. Bube and H. E. MacDonald : Phys. Rev. 121, 473 (1961)
11) H. J. Juretschke, R. Landauer and J. A. Swanson : J. Appl. Phys. 27, 838 (1956)
12) M. Bertolotti, T. Papa, D. Sette and G. Vitali : J. Appl. Phys. 38, 2645 (1967)
13) R. R. Holmes : IEEE Trans. NS-17, 137 (1970)

(昭和51年1月10日受付)